Oxidation of glucose and arabinose mixtures over Au/Al$_2$O$_3$

Sebastian Franz[1] · Nataliya D. Shcherban[2] · Irina L. Simakova[3] · Markus Peurla[4] · Kari Eränen[1] · Johan Wärnå[1] · Tapio Salmi[1] · Dmitry Yu. Murzin[1]

Abstract

Oxidation of a mixture of glucose and arabinose over 1% Au deposited on alumina was investigated in a semi-batch reactor varying pH, temperature and partial pressure of oxygen. Elevation of the latter enhancing the rate induced also losses in selectivity to aldonic acids. A kinetic model representing the catalytic oxidation reactions of arabinose and glucose along with respective isomerization to fructose and ribulose was developed. Calculations based on the model were able to describe experimental data in a reliable way.

Keywords Sugar oxidation · Gold catalysts · Glucose · Arabinose · Kinetic modelling

Introduction

Supported gold nanoparticles being highly active and selective low-temperature catalysts in the oxidation of carbon monoxide, carbohydrates and aldehydes [1–7] have also demonstrated a superior durability due to high resistance to deactivation, which is typically caused by over-oxidation and poisoning of the active metal phase [8]. It has been shown that alumina supported gold nanoparticles exhibit a high catalytic activity in the oxidation of sugar molecules under mild reaction conditions [9, 10].

✉ Dmitry Yu. Murzin
dmurzin@abo.fi

[1] Laboratory of Industrial Chemistry and Reaction Engineering, Johan Gadolin Process Chemistry Centre, Åbo Akademi University, Biskopsgatan 8, Abo, 20500 Turku, Finland

[2] L.V. Pisarzhevsky Institute of Physical Chemistry, National Academy of Sciences of Ukraine, 31 pr. Nauky, Kiev 03028, Ukraine

[3] Boreskov Institute of Catalysis, Lavrentieva ave. 5, Novosibirsk, Russia 630090

[4] University of Turku, 20500 Turku, Finland

Structure sensitivity for the oxidation reactions has been observed implying that the size of the gold nanoparticles influences the catalytic activity [5, 11]. For example in the oxidation of arabinose the maximum of catalytic activity was reported to be at the gold cluster size of ca. 2.5 nm [10].

Utilization of natural resources such as lignocellulosic biomass for the catalytic transformation of monomeric and oligomeric sugars into value-added products attracts an increasing attention complying with sustainable development [12, 13]. For instance, the hemicellulose arabinogalactan, which appears in large amounts in *Larix sibirica*, can be selectively converted to arabinose and galactose monomers via acid-catalyzed hydrolysis. Both homogeneous and heterogeneous catalysts can be used as discussed in [14]. The sugar monomers can be transformed catalytically to valuable products by hydrogenation, isomerization or oxidation. In the latter case aldonic acids are formed. Inexpensive and environmentally friendly oxidants such as air or molecular oxygen and noble metal catalysts such as gold allow achieving high selectivity towards the desired aldonic acids under mild conditions [10, 11].

Aldonic acids have found a wide application in the alimentary and detergent industries as well as in medicine and cosmetics [15]. Moreover, carbohydrate-based products are preferable due to their biodegradability and biocompatibility [13]. Therefore, selective oxidation of carbohydrates into valuable sugar acids is of significance considering the broad application range.

It should be pointed out that oxidation of both glucose and arabinose separately has been intensively investigated in the literature [16–18]. The detailed kinetic studies devoted to the hydrogenation of sugar mixtures should be mentioned [19, 20]. At the same time, according to our knowledge no articles in the open literature devoted to selective oxidation of sugars mixtures have been published. Such an oxidation process is, however, important due to a necessity of utilization not only individual sugars but also sugar mixtures obtained by hydrolysis of carbohydrate polymers.

The aim of the current work was to investigate oxidation of the model glucose and arabinose mixtures over gold nanoparticles supported on alumina. The authors did not have any specific type of biomass in mind because the intention was to use a model mixture of five and six carbon sugars with close initial concentrations. Such approach was adopted to mitigate a potential influence of different sugar concentrations characteristic of real biomass.

The influence of such parameters as temperature, pH, oxygen pressure, catalyst mass and sugar ratios was explored in detail and the performance of the mixtures was compared with oxidation of individual sugars. Finally, a kinetic model was proposed based on a feasible reaction mechanism and tested against the experimental data.

Experimental

Catalyst preparation

Alumina supported gold catalyst (Au/Al_2O_3) previously reported to be highly active in sugar oxidation was prepared according to the deposition–precipitation method

described in ref. [21]. The alumina support was added as a powder to a 1.6×10^{-3} M aqueous solution of $HAuCl_4$ with urea (0.21 M) heated up to 81 °C. The suspension of $HAuCl_4$, urea and Al_2O_3 was mixed under heating at 81 °C for 4 h and filtered. Afterwards, the catalyst was washed with water and additionally with a NH_4OH solution for the removal of excess chloride after the deposition of gold onto the support. After further washing with deionized water and filtering, the catalyst was dried at room temperature for 24 h. Finally, the catalyst was pretreated under an airflow with an increasing temperature ramp of 2 °C/min until 350 °C.

Catalyst characterization

Nitrogen adsorption was measured by a volumetric method (77 K, up to 1 atm) using Sorptomatic 1990 (Thermo Electron Corp.). Prior to the measurements, the samples were evacuated ($P \leq 0.7$ Pa) at 300 °C for 4 h. The specific surface area (S_{BET}) was evaluated by BET equation [22], and the mesopore diameters were determined from the desorption branches of the isotherm, using the method of Barret-Joyner-Hallenda (BJH) [23].

TEM images were obtained using the field emission TEM JEM-2100F (JEOL) with an accelerating voltage of 200 kV. A sample was dispersed in ethanol in an ultrasonic bath for 5 min, and then the suspension was deposited to a copper grid coated with a carbon film. The particle size distribution (PSD) was determined by manually measuring d_p for over 300 Au particles from at least six different positions, which also was used for calculating the mean particle size ($\overline{d_p}$).

Catalytic tests

Oxidation experiments of glucose and arabinose mixtures were carried out in a laboratory-scale glass reactor equipped with a heating jacket and an efficient mechanical stirrer. The experiments were conducted in a semi-batch mode under a constant gas flow of oxygen in argon. A Brooks 5850S device was used to control and adjust the gas feed. Temperature and pH were controlled with a Metrohm Titrando 907 device equipped with a Metrohm Unitrode electrode.

The reactor was flushed with around 65 ml/min argon and heated to the desired reaction temperature. During flushing, the dry catalyst with particle sizes less than 65 μm was inserted into the reactor. Experiments with different catalyst bulk densities in the reactor were conducted to ensure that the productivity is proportional to the catalyst loading and thus the reaction is not limited by gas–liquid mass transfer. The majority of kinetic experiments were performed with the catalyst bulk density 0.66 g/l. The very small catalyst particles were used to suppress the internal mass transfer limitations in the catalyst pores. Simultaneously, the sugar solution of L-arabinose (Sigma-Aldrich, $\geq 99\%$) and anhydrous D-glucose (Fluka, $\geq 98\%$) with the sugar mass ratio 1:1 was heated to approximately 40–50 °C under vigorous stirring to minimize the temperature difference in the beginning of the experiment. The solution contained in all cases a total amount of 2 g/100 ml sugar dissolved in deionized water with a total volume of 150 ml. Once the reactor vessel had been completely

flushed, the sugar solution was poured into the reactor and heated in argon atmosphere to the desired reaction temperature under stirring and pH control. A high agitation rate of 1000 rpm was used to diminish the influence of external mass transfer limitations. Upon reaching the reaction temperature, the argon flow was reduced to the value used in the reaction and the pre-adjusted oxygen was introduced into the argon flow, resulting in a total gas flow of 40 ml/min. The pH was controlled by addition of 1 M NaOH. Otherwise formation of the acid will result in the pH drift influencing the results, as it is known that pH has a strong influence on the oxidation kinetics [10, 24].

During the experiments, the samples were withdrawn from the liquid phase and the concentration profiles of the reactants and the reaction products were monitored using high precision liquid chromatograph (VWR Hitachi Chromaster) equipped with a 300×7.8 mm Bio-Rad Aminex HPX-87C column and a RI detector (VWR Hitachi Chromaster 5450). The operating temperature of the column was set to 80 °C and the flow rate 0.6 ml/min using 1.2 mM $CaSO_4$ as the eluent, resulting in a column backpressure ranging between 65 and 70 bar. The injection volume of the sample was set to 10 μl.

Potential leaching of metal particles into the liquid phase during the reaction was investigated by inductively coupled plasma mass spectrometry (ICP-MS, PerkinElmer, Elan 6100 DRC Plus). The liquid samples, placed in a PTFE vessel, were dissolved in aqua regia solution in a microwave oven (Anton Paar, Multiwave 3000). Subsequently, the samples were diluted with water, first to 100 ml and then further to volumetric ratio 1:5. The acids used for the aqua regia solution were of Suprapur® grade (30% HCl, Merck; 65% HNO_3, Merck). For calibration, a commercial multielement standard was used.

The current work was focused on catalyst screening and kinetic modelling, while stability of the catalyst was considered outside of the scope deserving a separate study, involving catalyst recycling. Such study was performed in the SpinChem rotating bed reactor with the gold on alumina catalyst in the form of extrudates and will be reported separately.

Results and discussion

Catalyst characterization

The surface area of the alumina support was 204 m^2/g remaining almost the same after deposition of gold. The pore volume of the catalyst is 0.5 cm^3/g with the average pore diameter of 10 nm.

According to the TEM measurements Au/Al$_2$O$_3$ possesses small gold nanoparticles (Fig. 1) with an average particle size of 2.2 nm.

The catalyst was also analyzed after an oxidation reaction of 1:1 arabinose—glucose mixture at 70 °C, pH 8 and oxygen pressure 0.125 atm. Prior to imaging, the catalyst was washed according to the method described in the experimental section. The PSD for the fresh and spent catalysts (Fig. S1) was almost the same.

Fig. 1 TEM-images for 1 wt% Au/Al_2O_3
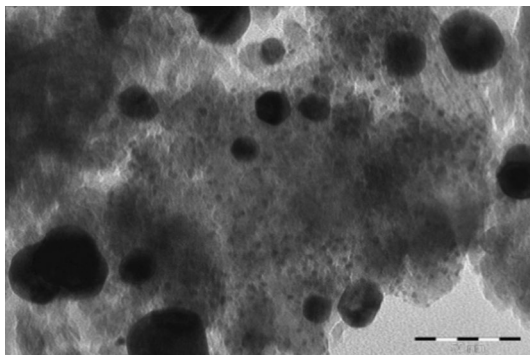
Oxidation of mixtures over gold on alumina catalysts: influence of reaction parameters

Selective oxidation of a mixture of glucose and arabinose to the corresponding aldonic acids (Fig. 2) was carried out isothermally at atmospheric pressure, in aqueous phase in semi-batch mode with the reactant introduced in a batch mode and the oxidant fed continuously.

Evaluation of the liquid-to-solid mass transport limitations and intraparticle diffusion limitations similar to [24] confirmed that the catalytic data were obtained in the kinetic regime.

As visible from Fig. 3 where the concentration curves are plotted against the normalized time, glucose and arabinose were oxidized to the corresponding aldonic acids, namely gluconic and arabinonic acids.

In experiments varying the ratios between arabinose and glucose the total sugar content was kept at 20 g/l. Mixtures with different molar ratios as well as individual sugars were investigated (Fig. S2). As a general observation following from Figs. 3 and S2, rather similar oxidation rates were observed for individual compounds and in mixtures, with oxidation of arabinose being slightly preferred.

A challenge in analysis of the oxidation of mixtures is a partial overlapping of the peaks of arabinose and fructose, thus preventing a full mass balance closure. For the experiments with only one sugar, there was no overlapping and selectivity towards the respective aldonic acids very high even if small quantities of keto sugars, i.e. fructose and ribulose were observed at low conversions for glucose and arabinose, respectively.

The influence of the reaction temperature at 50–80 °C on the oxidation kinetics can be elucidated from Figs. 3 and S3. Besides a typical increase in the catalytic activity with temperature according to the Arrhenius equation, the mutarotation equilibrium is slightly shifted with temperatures towards a higher furanose fraction, hence giving a higher fraction of the reactive compounds. On the other hand, the gas–liquid solubility is less favourable as the temperature is elevated [25]. This seems to be the reason for the observed experimental data.

While in ref. [24] a significant impact of pH was observed for arabinose oxidation, in the current work no major influence of pH on the reaction rate and product
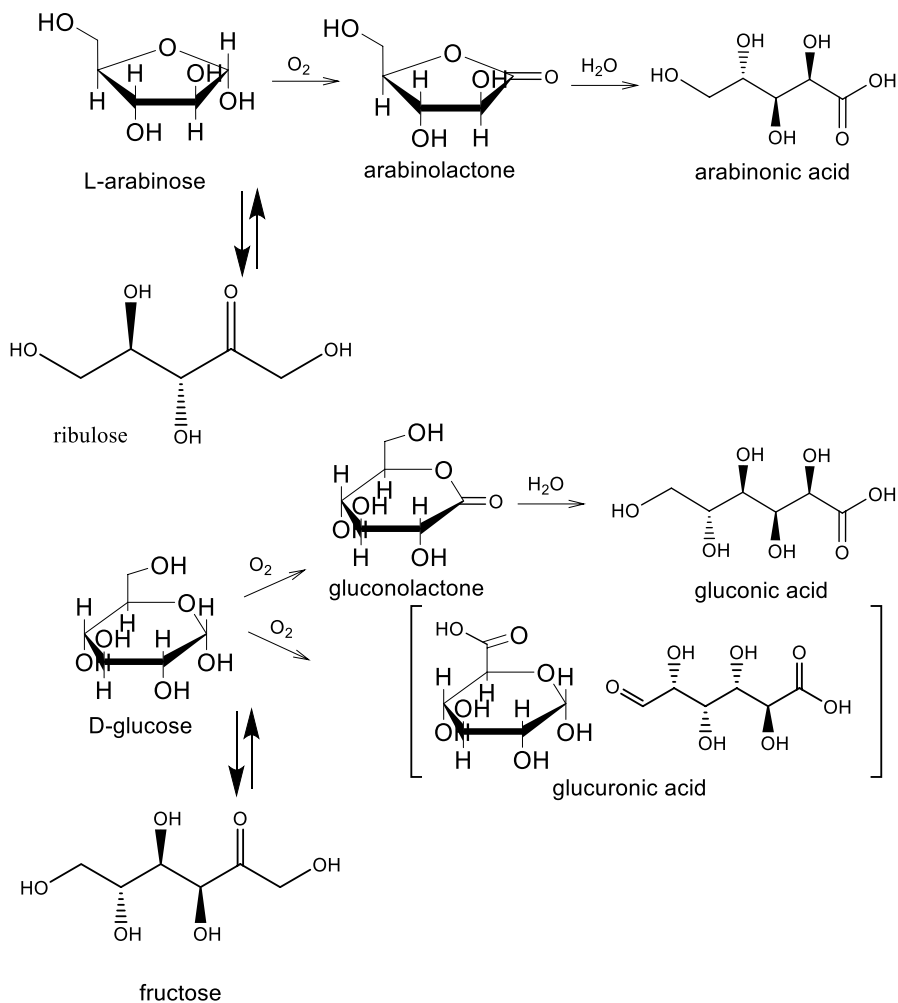
Fig. 2 Oxidation of arabinose (**a**) and glucose (**b**) over supported gold catalysts

distribution was noticed. For arabinose, pH 8 and 9 displayed close to identical results, while the reaction proceeded slightly less slowly at pH 7 (Fig. 4). Glucose oxidation exhibited similar results, where the rates at pH 8 and 9 were almost identical being slightly higher than at pH 7.

It has earlier been mentioned that gold contrary to Pd does not undergo over-oxidation and thus, an excess in oxygen should not induce catalyst deactivation. However, because of oxygen adsorption on the active sites an excessive concentration of oxygen might lead to lower availability of active sites to sugar molecules, diminishing the oxidation rate.

To investigate the influence of oxygen pressure on the reaction, three experiments with varying oxygen pressures were carried out (Fig. 5).
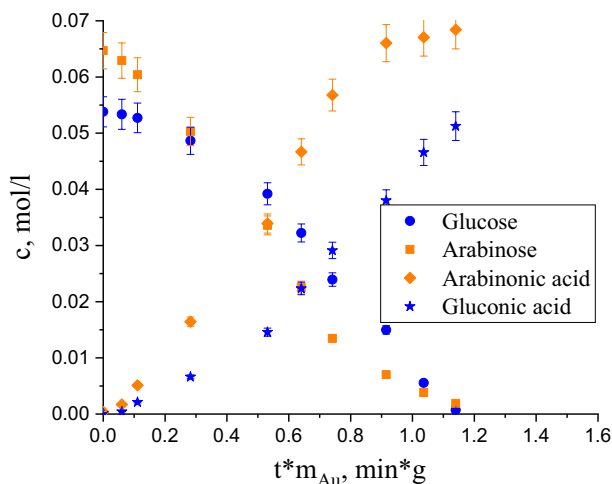
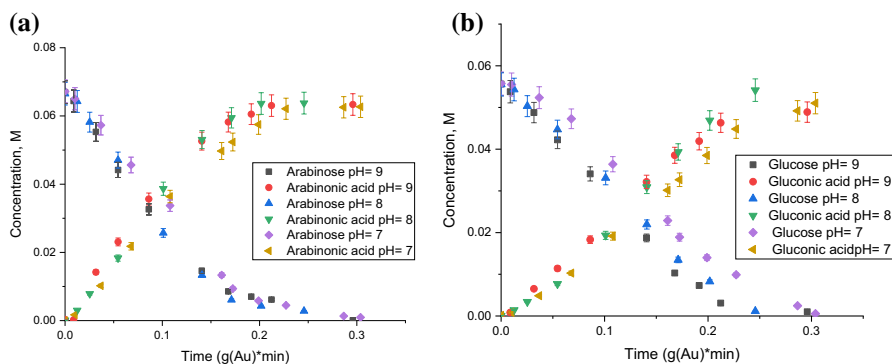**Fig. 3** Kinetic curves for oxidation of the glucose and arabinose mixture over 1 wt% Au/Al$_2$O$_3$. Conditions: 70 °C, pH 8, pO$_2$ = 0.125 atm

Fig. 4 Oxidation of 1:1 arabinose–glucose mixtures over 1% Au/Al$_2$O$_3$ at different pH values and 70 °C, pO$_2$ = 0.125 atm, m$_{cat}$ = 0.1 g (catalyst bulk density 0.66 g/L). For illustrative purposes, the two sugars are shown in separate graphs, **a** arabinose, **b** glucose

While the oxygen concentration increases linearly, the oxidation rates of arabinose and glucose do not follow the same trend. Minor changes of the rates at oxygen pressures over 0.125 bar are a clear indication that mass transfer of oxygen is not the rate-limiting factor. Overlapping of the curves at the pressure of oxygen equal to 0.125 and 0.25 bar means that the reaction rate approaches a zero order in oxygen.

Kinetic modelling

A detailed kinetic model for catalytic arabinose oxidation partially based on the previous work [9] has been discussed more recently [18]. Complexity of the model in [18] reflected a need to describe the pH dependence observed in [9] for experiments
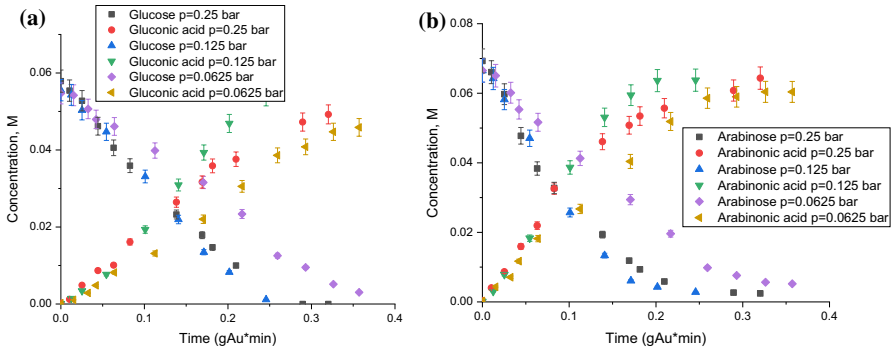
Fig. 5 Oxidation of 1:1 arabinose–glucose mixtures over 1% Au/Al$_2$O$_3$ at different oxygen pressures and 70 °C, pH 8 and m$_{cat}$=0.1 g (catalyst bulk density 0.66 g/L). For illustrative purposes, the sugars are displayed in separate graphs **a** glucose, **b** arabinose

performed in shaker. In the current work such dependence was marginal, thus a certain simplification could be done. The reaction network can be reduced to oxidation (reactions 1 and 2) of glucose and arabinose to gluconic and arabinonic and isomerization (reactions 3 and 4) of glucose and arabinose to fructose and ribulose. The rate equations are thus:

$$r_1 = \frac{k_1 c_{Glucose} c_{O_2}}{\left(1 + K_{Glucose} c_{Glucose} + K_{Arabinose} c_{Arabinose} + K_{O_2} c_{O_2}\right)^2} \tag{1}$$

$$r_2 = \frac{k_2 c_{Arabinose} c_{O_2}}{\left(1 + K_{Glucose} c_{Glucose} + K_{Arabinose} c_{Arabinose} + K_{O_2} c_{O_2}\right)^2} \tag{2}$$

$$r_3 = \frac{k_3 c_{Glucose}}{\left(1 + K_{Glucose} c_{Glucose} + K_{Arabinose} c_{Arabinose} + K_{O_2} c_{O_2}\right)} \tag{3}$$

$$r_4 = \frac{k_4 c_{Arabinose}}{\left(1 + K_{Glucose} c_{Glucose} + K_{Arabinose} c_{Arabinose} + K_{O_2} c_{O_2}\right)} \tag{4}$$

here r_1 and r_2 reflect the rates of the oxidation reactions for glucose and arabinose, respectively, and r_3 and r_4 correspond to isomerization of glucose and arabinose to respectively fructose and ribulose. Surface reactions between adsorbed sugars and oxygen were considered to be the rate limiting in oxidation in the spirit of the Langmuir–Hinshelwood mechanism. Isomerization of adsorbed sugars was considered the step defining the rates of isomerization reactions. As can be easily seen from Eqs. 1–4, the rate constants are merged ones comprising also adsorption coefficients of sugars (glucose for k_1 and k_3, arabonose for k_2 and k_4) and oxygen (for k_1 and k_2).

Because the peaks of arabinose and fructose in the chromatograms overlapped, the concentration of arabinose is described by

$$c_{Arabinose} = c_X - c_{Glucose,0} + c_{Glucose} + c_{Gluconicacid} \tag{5}$$

Here $c_{Glucose,0}$ reflects the initial glucose concentration. Parameter c_X defines the combined concentration of arabinose and fructose.

Finally, the mass balances of the components can be defined with the differential equations

$$\frac{dc_{Glucose}}{dt \cdot m_{cat}} = -r_1 - r_3 \tag{6}$$

$$\frac{dc_{Gluconate}}{dt \cdot m_{cat}} = r_1 \tag{7}$$

$$\frac{dc_X}{dt \cdot m_{cat}} = -r_2 - r_4 + r_3 \tag{8}$$

$$\frac{dc_{Arabinonate}}{dt \cdot m_{cat}} = r_2 \tag{9}$$

$$\frac{dc_{ribulose}}{dt \cdot m_{cat}} = r_4 \tag{10}$$

Catalyst deactivation was not included in the model, because in addition to absence of sintering according to TEM (Fig. 1), analysis of the spent catalysts by ICP-MS suggested just a minor catalyst leaching (ca. 4% of the initial gold content).

In the non-linear regression analysis, the unknown parameters were thus the rate constants k_1–k_4, the adsorption constants $K_{Glucose}$, $K_{Arabinose}$ and K_{O_2}, and the activation energies $E_{a,1}..E_{a,4}$. All kinetic constants k_i were considered to be dependent on temperature according to

$$k_i = A_i e^{\frac{-E_{act}}{R}\left(\frac{1}{T} - \frac{1}{T_{ave}}\right)} \tag{11}$$

Here k_i, A_i, E_{act}, R, T and T_{ave} denote the reaction rate constant, the reaction rate constant at the average temperature (70 °C or 343 K), activation energy of the reaction, the universal gas constant, the reaction temperature and the average temperature, respectively.

Temperature dependent solubility of oxygen was calculated from

$$c_{O_2} = p_{O_2} e^{\frac{0.0467T^2 + 203.35 Tln\left(\frac{T}{298}\right) - (299.378 + 0.092T)(T - 298) - 20.591 \cdot 10^3}{8.3144T}} \tag{12}$$

here temperature T is in Kelvin (K).

The parameter estimation was carried out numerically solving the differential Eqs. (6)–(10) with the backward difference method using the software ModEst [26]. All data sets were fitted together in the parameter estimation. The best parameter estimation is achieved by minimizing the residual sum of squares

$$Q = \sum (c_{i(est)} - c_{i(exp)})^2 \qquad (13)$$

here c and i denote the concentrations and the corresponding reactants. The combined simplex-Levenberg–Marquardt method was used to minimize the objective function. Three examples of data fitting along with the parity plot are shown in Fig. 6, while all the results are provided in Fig. S4. Important to note is that the experiment with oxygen pressure 0.250 atm gave deviations from the experimental data as the mass balance closure was inadequate.

Nevertheless, the results demonstrated a reliable fit to the experimental data with a 97.3% degree of explanation and the values of parameters presented in Table 1, while the correlation matrix of parameters in given in Table 2. It follows from Table 1 that the majority of parameters are relatively well-defined from the statistical viewpoint. Low values of the apparent activation energies are most probably related to the lumped character of the rate constants in Eqs. 1–4 reflecting also heats of adsorption of sugars and oxygen on the surfaces of gold catalysts. Such values are, however, in line with the lumped value for the activation energy of arabinose
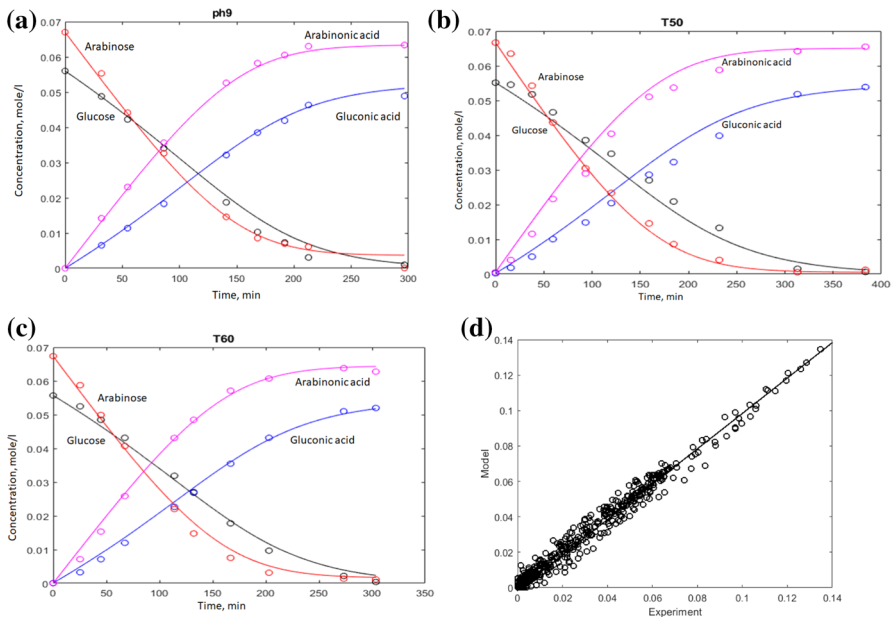

Fig. 6 Comparison between experimental and calculated data for 0.1 g of 1% Au/Al$_2$O$_3$ catalyst at **a** 70 °C, pO$_2$=0.125 atm, 1:1 mass ratio arabinose–glucose and pH=9, **b** 50 °C, pO$_2$=0.125 atm, 1:1 mass ratio arabinose–glucose and pH=7, **c** 60 °C, pO$_2$=0.125 atm, 1:1 mass ratio arabinose–glucose and pH=7, and **d** the parity plot comprising data a all conditions. The lines represent calculated values

Table 1 Results from parameter estimation for oxidation of arabinose–glucose mixtures

Parameter	Estimated value	Relative standard error (%)	Units
A_1	0.15×10^5	23	l/mol min g
A_2	0.3×10^5	23	L/mol min g
A_3	0.025	20	Min/g
A_4	0.03	21	Min/g
K_{Ara}	39	14	l/mol
K_{Gluc}	20	17	l/mol
K_{O2}	0.175×10^5	15	l/mol
$E_{a,1}$	10	25	kJ/mol
$E_{a,2}$	6	33	kJ/mol
$E_{a,3}$	81	27	kJ/mol
$E_{a,4}$	24	> 100	kJ/mol

k_i lumped rate constants, K_i adsorption equilibrium constants, $E_{a,i}$ activation energies

Table 2 Correlation matrix of parameters

	k_1	k_2	k_3	k_4	K_{Ara}	K_{Gluc}	K_{O2}	$E_{a,1}$	$E_{a,2}$	$E_{a,3}$	$E_{a,4}$
k_1	1										
k_2	0.988	1									
k_3	0.709	0.732	1								
k_4	0.650	0.677	0.599	1							
K_{Ara}	0.959	0.983	0.740	0.712	1						
K_{Gluc}	0.949	0.934	0.693	0.640	0.933	1					
K_{O2}	0.972	0.966	0.672	0.612	0.908	0.860	1				
$E_{a,1}$	-0.023	-0.060	-0.020	-0.043	-0.064	0.002	-0.058	1			
$E_{a,2}$	-0.113	-0.074	-0.070	-0.024	-0.055	-0.133	-0.101	-0.374	1		
$E_{a,3}$	-0.078	-0.097	-0.458	-0.137	-0.111	-0.087	-0.071	0.020	0.114	1	
$E_{a,4}$	-0.036	-0.036	-0.075	-0.130	-0.044	-0.045	-0.026	-0.153	0.004	0.162	1

oxidation reported previously [18] for the data generated using a gold catalyst in a reactor operating in a shaking mode [10].

A relatively high standard deviation of the parameter value for the activation energy in isomerization of arabinose to ribulose is related to the minor amount of the latter. A higher value of the adsorption equilibrium constant for arabinose confirms that arabinose adsorption is more favoured than glucose. Furthermore, a more significant effect of temperature on arabinose oxidation is also confirmed by a slightly higher activation energy value compared to glucose. A high value of the adsorption coefficient for oxygen reflects the low concentration of oxygen in aqueous solutions.

Table 2 illustrates correlations between parameters with value close to unity indicating that the parameter values are unreliable. The highest correlation found

is 0.99, while most of the correlations are significantly lower being thus statistically satisfying. High correlations between parameters can be related to difficulties in, for example, reliable estimation of the adsorption parameters based on available experimental data set.

To verify reliability of parameters the statistical analysis was conducted using the Monte Carlo Markov Chain (MCMC) method [27] incorporated in the optimization software ModEst. This method allows evaluation of the probability distribution of parameters [28]. The results of the analysis presented in Fig. S5 illustrate that, apart from the adsorption coefficient of oxygen, other parameters exhibit rather well defined maxima in the posterior distributions of parameters. Such distributions reflect their probability with the most probable values of constants being at maxima. Fig. S5 indicates that even the value of the activation energy for the step 4 from Table 1 is estimated in a statistically reliable way. Insignificant dependence on the oxygen pressure when the pressure is elevated is apparently the reason for the broad probability distribution vs the parameter value for the oxygen adsorption constant (Fig. S5).

Conclusions

Oxidation of binary mixtures of glucose and arabinose over gold particles supported on alumina was studied in the temperature range 50–80 °C in a semi-batch mode. Oxidation reactions of arabinose–glucose mixtures over 1% Au/Al_2O_3 demonstrated that under all studied conditions oxidation of arabinose is more favourable compared to that of glucose. Upon elevation of oxygen pressure the reaction rate displayed a zero order dependence in the oxygen. The influence of pH on the reactivity was marginal, while the effect of temperature was more pronounced, leading to the rate maximum at 70 °C. Higher temperatures exceeding 70 °C and pH values above 8 apparently enhance formation of by-products (e.g. keto-sugars), especially for glucose oxidation.

No sintering was observed according to TEM while leaching was minor based on ICP-MS of the spent catalyst.

A kinetic model was developed which took into account the oxidation of sugars as well aldo-ketose isomerization. The rate limiting reactions in oxidation were surface reactions between adsorbed sugars and oxygen. Numerical data fitting was performed for all data sets simultaneously comprising data for individual components and the binary mixtures at different operation conditions. The model is able to explain the experimental data on oxidation of arabinose and glucose mixtures at different ratios between the sugars, temperature, pH and oxygen pressure in a reliable way. Statistical analysis using the Monte Carlo Markov Chain method was performed confirming statistical reliability of the parameter estimates.

References

1. Haruta M (2003) When gold is not noble : catalysis by nanoparticles. Chem Rec 3:75
2. Haruta M (2004) Nanoparticulate gold catalysts for low-temperature CO oxidation. J New Mater Electrochem Syst 7:163
3. Lopez N, Janssens TVJ, Clausen BS, Xu Y, Mavrikakis M, Bligaard T, Norskov JK (2004) On the origin of the catalytic activity of gold nanoparticles for low-temperature CO oxidation. J Catal 223:232
4. Biella S, Prati L, Rossi M (2002) Selective oxidation of D-glucose on gold catalyst. J Catal 206:242
5. Ishida T, Kinoshita N, Okatsu H, Akita T, Takei T, Haruta M (2008) Influence of the support and the size of gold clusters on catalytic activity for glucose oxidation. Angew Chem Intern Ed 47(48):9265
6. Corma A, Domine ME (2005) Gold supported on a mesoporous CeO_2 matrix as an efficient catalyst in the selective aerobic oxidation of aldehydes in the liquid phase. Chem Commun 36:4042
7. Hashmi ASK (2007) Gold-catalyzed organic reactions. Chem Rev 107:3180
8. Mirescu A, Prüße U (2007) A new environmental friendly method for the preparation of sugar acids via catalytic oxidation on gold catalysts. Appl Catal B 70:644
9. Kusema BT, Murzin DYu (2013) Catalytic oxidation of rare sugars over gold catalysts. Catal Sci Technol 3:297
10. Kusema BT, Campo BC, Simakova OA, Leino A-R, Kordas K, Mäki-Arvela P, Salmi T, Murzin DYu (2011) Selective oxidation of arabinose to arabinonic acid over Pd-Au catalysts supported on alumina and ceria. ChemCatChem 3:1789
11. Haruta M (1997) Size- and support-dependency in the catalysis of gold. Catal Today 36:153
12. Chheda JN, Huber GW, Dumesic JA (2007) Liquid-phase catalytic processing of biomass-derived oxygenated hydrocarbons to fuels and chemicals. Angew Chem Int Ed 46:7164
13. Baatz C, Prüße U (2007) Preparation of gold catalysts for glucose oxidation. Catal Today 122:325
14. Kusema BT, Xu C, Mäki-Arvela P, Willför S, Holmbom B, Salmi T, Murzin DY (2010) Kinetics of acid hydrolysis of arabinogalactans. Intern J Chem React Eng 8:A44
15. Ishida T, Watanabe H, Bebeko T, Akita T, Haruta M (2010) Aerobic oxidation of glucose over gold nanoparticles deposited on cellulose. Appl Catal A 377:42
16. Wang Y, Van de Vyver S, Sharma KK, Román-Leshkov Y (2014) Insights into the stability of gold nanoparticles supported on metal oxides for the base-free oxidation of glucose to gluconic acid. Green Chem 16:719
17. Simakova OA, Kusema BT, Campo BC, Leino AR, Kordás K, Pitchon V, Murzin DY (2011) Structure sensitivity in L-arabinose oxidation over Au/Al_2O_3 catalysts. J Phys Chem C 115:1036
18. Correia LS, Grénman H, Wärnå J, Salmi TO, Murzin DY (2019) Catalytic oxidation kinetics of arabinose on supported gold nanoparticles. Chem Eng J 370:952

19. Wisnlak J, Simon R (1979) Hydrogenation of glucose, fructose and their mixtures. Ind Eng Chem Prod Res Dev 18:50
20. Sifontes Herrera VA, Saleem F, Kusema B, Eränen K, Salmi T (2012) Hydrogenation of L-arabinose and D-galactose mixtures over a heterogeneous Ru/C catalyst. Top Catal 55:550
21. Smolentseva E, Kusema BT, Beloshapkin S, Estrada M, Vargas E, Murzin DY, Simakov A (2011) Selective oxidation of arabinose to arabinonic acid over Pd–Au catalysts supported on alumina and ceria. Appl Catal A 392:69
22. Brunauer S, Emmett PH, Teller E (1938) Adsorption of gases in multimolecular layers. J Am Chem Soc 60:309
23. Barrett EP, Joyner LG, Halenda PP (1951) The determination of pore volume and area distributions in porous substances. I. Computations from nitrogen isotherms. J Am Chem Soc 73:373
24. Kusema BT, Campo BC, Mäki-Arvela P, Salmi T, Murzin DY (2010) Selective catalytic oxidation of arabinose—a comparison of gold and palladium catalysts. Appl Catal A 386:101
25. Tromans D (1998) Temperature and pressure dependent solubility of oxygen in water: a thermodynamic analysis. Hydrometallurgy 48:327
26. Haario H (2011) ModEst user's guide, Helsinki
27. Görlitz L, Gao Z, Schmitt W (2011) Statistical analysis of chemical transformation kinetics using Markov-Chain Monte Carlo methods. Environ Sci Technol 45:4429
28. Fuller EN, Schettler PD, Giddings JC (1966) New method for prediction of binary diffusion coefficients. Ind Eng Chem 58:18

Publisher's Note Springer Nature remains neutral with regard to jurisdictional claims in published maps and institutional affiliations.